Active Mesh for Minimal Surface Problems

Cheng-Yuan Liou & Quan-Ming Chang

Department of Computer Science and Information Engineering,
National Taiwan University, Taipei, Taiwan, R.O.C.
Tel: 8862-3625336 ext 515, Fax: 8862-3628167, Email: cyliou@csie.ntu.edu.tw.

Abstract

We present an economic and efficient technique to reach minimal surface. This technique can facilitate many computer-aided-designs in obtaining desired surfaces. Potts type networks are formulated for active meshes (Liou 96 & 97) which are used to emulate soap films. These meshes will reduce their areas according to the surface energies which are proportional to the surface areas. Several simulations are carried out, such as the catenoid, helicoid.

Keywords: soap film, Hopfield network, active mesh, minimal surface, mean field annealing.

1 The discrete surface

The problem of finding minimal surfaces is one of the deeper problems of the calculus of variations. This problem has been called Plateau's problem in honor of the Belgian physicist, Plateau (1801–1883). In its simple form, it can be stated as: *What is surface of smallest area bounded by a given closed curve (contour) in space ?*

Mathematically, Plateau's problem is formulated with a partial differential equation, or a system of such equations (Courant and Robbins 1941). All (non-plane) minimal surfaces must be saddle-shaped and the mean curvature, H, at every point must be zero. The mean curvature is the average of the principal curvatures (Hoffman and Meeks 1990).

A minimal surface is a mathematician's idealization of soap film (Callahan and Hoffman 1988). In this work, we present a new approach to solve this problem using the active mesh (Liou 96 & 97), which is devised to emulate the soap film. This discrete surface is a topological complex consisting of quadrilaterals. The mesh is formulated with a Hopfield network and is further controlled by a Potts type network (Wu 1982) to tension the mesh smoothly, collectively, and distributively. The energy of the network is proportional to the surface area. When the minimun is reached, the minimal surface is obtained. Note that Brakke (1992) proposes a Surface Evolver which represents a soap film surface as a simplicial complex consisting of vertices, edges and facets. The Surface Evolver uses a finite-element method to obtain the minimal surface which works in a way of global descent of total strain energy. Our method is rather collective and distributive which follows the behaviour of soap films. The mesh (Liou 96, & 97) can shrink successfully to a Steiner tree with two Steiner points when we nail down the four corners of a square mesh and release the rest of the mesh. To our knowledge, this success has not been reported from using other elegant elastic surface methods or finite-element based methods to emulate the soap film. We now extend this mesh to 3D and test its behaviour in reaching minimal surface.

Suppose that a surface is discretized and has many nonoverlapping quadrilateral units. The area of the surface can be approximated by summing all unit areas. Consider a square unit with side length x. The area of a square unit is x^2. If the boundary sides of this unit are taken as springs and the natural lengths of these springs are zero, then the strain energy of these four springs is

$$E_{spring} = 4 * (\tfrac{1}{2}\alpha x^2) = 2\alpha x^2 \propto x^2$$
$$, \alpha \text{ is the spring constant}$$

We can see that the energy is proportional to the unit area, *which is also the case for soap film.*When we minimize the energy, we minimize the area at the same time. In fact, the springs state that each unit resembles a closed snake (Kass et al. 1987). We will use the snake model for each unit and build the mesh. Note that for a rectangular soap film the total surface tension along one side of its boundary is proportional to the length of the side and normal to the side. The net forces exert by this unit on its neighbors can be properly represented by these four springs when these units are dense enough.

2 The units of mesh

Each unit of the mesh is taken as a snake. The shape of a snake is controlled by internal forces and external forces.If we represent the position of a snake parametrically by $\mathbf{p}(c) = (x(c), y(c), z(c))$, the spring energy function can be written as

$$E^*_{snake} = \int_0^1 [(\alpha(c)|\,\mathbf{p}'(c)\,|^2)/2]dc \qquad (1)$$

where $\alpha(c)$ is spring constant. We discretize this energy function

$$E'_{snake} = \sum_{i=1}^{n} \alpha_i \mid \mathbf{p}_i - \mathbf{p}_{i-1} \mid^2 \qquad (2)$$

where n is the number of snake points (or nodes), and $\mathbf{p}_i$ is the position of the ith snake point. Note that the snake in our model is a closed curve, and the 4 edges connecting the 4 points enclose a square area roughly.

Basing on the techniques presented in (Tsai et al. 1993; Williams and Shah 1992), we design a Potts neural network to minimize this discretized energy. The network consists of n mutually interconnected neurons, where n is the number of snake points. Each neuron corresponds to a snake point, and has m states which corresponds to m positions along m directions of the movements of this snake point (Figure 1). Note $m = 27$ in this 3D case. The energy function is computed at $\mathbf{p}_i$ and each of its 26 neighbors. The position (along a direction) having the smallest value of energy is chosen as the new position of $\mathbf{p}_i$ (Figure 1). This computation is accomplished implicitly by the Potts network. The output (state) of ith Potts neuron is indicated by a unit vector in a m-dimension vector space, $\mathbf{s}_i = (0, ..., 1, ..., 0)^T_{m*1}$. Each component of it is denoted as $s_{i,p}$ ($s_{i,p} = 0$ or 1). For the ith vector, the component $s_{i,p}$ with firing state 1 ($s_{i,p} = 1$) indicates the new position for the ith snake point with lowest energy. The Potts neuron must automatically satisfy the constraint $\sum_{p=1}^{m} s_{ip} = 1$. Under this constraint, the snake energy function with Potts neural network is formulated as

$$\begin{aligned} E_{snake} \\ = \quad & \sum_{i=1}^{n}\{w_1[(\sum_{p=1}^{m} x_{i,p}s_{i,p} - \sum_{p=1}^{m} x_{i-1,p}s_{i-1,p})^2 \\ + \quad & (\sum_{p=1}^{m} y_{i,p}s_{i,p} - \sum_{p=1}^{m} y_{i-1,p}s_{i-1,p})^2]\} \end{aligned} \qquad (3)$$

Note that α_i in (1) is taken as constant for homogeneous snakes and is included in a new constant w_1. w_1 is a scale factor and can be discarded.

3 The mesh

The homogeneous mesh is composed of many quadrilateral units (Figure 2). Thus, if we have $N = row * col$ nodes in the mesh, we'll have $Sn = (row - 1) * (col - 1)$ snakes. In the mesh model, we use "node", instead of using "snake point", to represent the configuration of the mesh. Each unit (snake) will shrink to a point if there is no constraint imposed upon it.

We can define the energy function for the mesh as $E_{mesh} = \sum_{i=1}^{Sn} E_{snake(i)}$, where Sn is the total number of snakes in the mesh and $E_{snake(i)}$ is defined in (3).

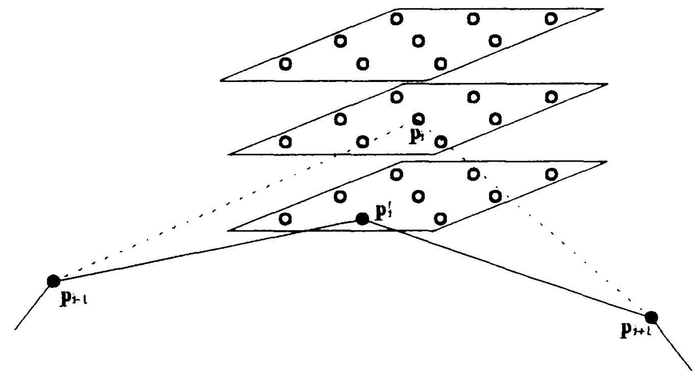

Figure 1. Each node of the mesh has 27 directions of movement.

E_{mesh} is minimized using the Potts neural network. When the network convergs, the minimal surface is found. To avoid getting stuck, keeping away from folding of the mesh, in local minima, the mean field theory (MFT) technique is applied. The discrete variable $s_{i,p}$ (or $\mathbf{s}_i$ in vector form) will be replaced by the corresponding continuous MFT variable $v_{i,p}$ (or $\mathbf{v}_i$ in vector form). That is $\mathbf{v}_i =< \mathbf{s}_i >_T$, where $< \mathbf{s}_i >_T$ denotes the average (mean) of $\mathbf{s}_i$ at temperature T. The Potts MFT equations for the mesh model is

$$\mathbf{u}_i = -\frac{1}{T}\frac{\partial E_{mesh}}{\partial \mathbf{v}_i}, \qquad \mathbf{v}_i = \mathbf{F}_N(\mathbf{u}_i) \qquad (4)$$

where T corresponds to the temperature in statistical mechanics. The vector-valued function $\mathbf{F}_N(\mathbf{u}_i)$ can be obtained using the saddle point method (Peterson and Söderberg 1989)

$$\mathbf{F}_N(\mathbf{u}_i) = \frac{\sum_{\mathbf{s}} \mathbf{s} e^{\mathbf{u}_i \mathbf{s}}}{\sum_{\mathbf{s}} e^{\mathbf{u}_i \mathbf{s}}}$$

Writing it out in components, we have

$$F_N^p(\mathbf{u}_i) = \frac{e^{u_{i,p}}}{\sum_b e^{u_{i,b}}}$$

It is obvious that this expression automatically satisfies the constraint $\sum_p F_N^p(\mathbf{u}_i) = 1$. Thus $\mathbf{v}_i$ automatically lies in the subspace $\sum_p v_{i,p} = 1$. From (4), we get

$$u_{i,p} = -\frac{1}{T}\frac{\partial E_{mesh}}{\partial v_{i,p}} = -\frac{1}{T}(\sum_j \sum_q W_{i,p;j,q} v_{j,q})$$

$W_{i,p;j,q}$ is derived as:

$$W_{i,p;j,q} = (W^{(1)} + W^{(2)}) * (x_{i,p}x_{j,q} + y_{i,p}y_{j,q})$$

where

$$\begin{aligned} W^{(1)} = \quad & \sum_{k=1}^{N}[-2w_1\alpha_{i,k}\phi_1(i,k) \\ & (2 - B(i)(k))](2 - \delta_{p,q})\delta_{i,j} \\ W^{(2)} = \quad & 4w_1\alpha_{i,j}\phi_1(i,j)[2 - B(i)B(j)] \end{aligned}$$

where $\delta_{i,j}$ is the Kronecker delta function. $\phi_1(i,j)$ and $B(i)$ are defined as:

$$l\phi_1(i,j) = \begin{cases} 1\text{,if i and j are parallel} \\ \text{neighborhood (Fig. 2).} \\ 0\text{,otherwise} \end{cases}$$

$$B(i) = \begin{cases} 1\text{,if node } i \text{ is a boundary node.} \\ 0\text{,otherwise} \end{cases}$$

The matrix, $W_{i,p;j,q}$, depends on the configuration of the mesh, and is recomputed at each iteration stage. All nodes are moved to new positions according to the converged states of the neurons within each stage. The paremeter w_1 is set to be a constant for homogeneous mesh during the evolution of the mesh. The temperature T starts from high temperature T_{high} and then reduces gradually to low termperature T_{low} within each stage.

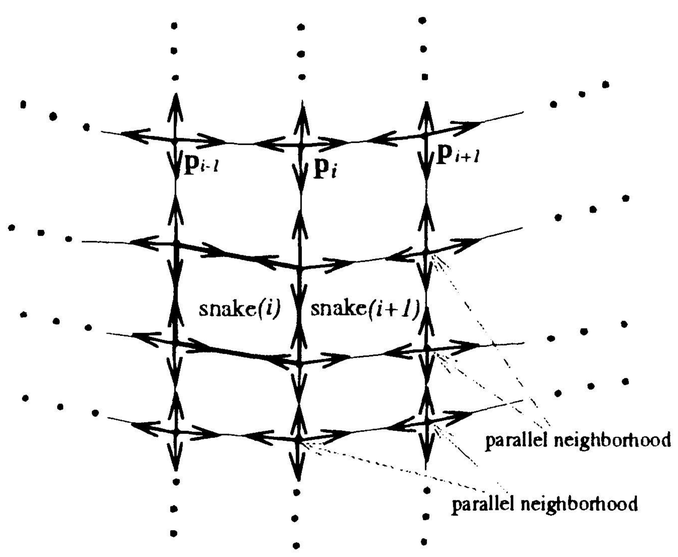

Figure 2. The mesh is composed of connected snakes. Each snake has four nodes in it.

4 Simulations & discussions

We now show how the mesh can be used to approach the minimal surface problem. The mesh is initialized skillfully to fit the fixed curves (boundaries) of the surface as shown in Figure 3(a). Then, the mesh will evolve to reach the minimal surface via the Potts neural network. During the evolution, the boundary of the mesh is fixed. Figure 3(b) shows the converged result of the mesh. Besides, converged shapes for four variations of the boundaries are provided in Figure 4.

Except for the plane, the helicoid is the only ruled minimal surface. It is a complete embedded minimal surface with finite topology and infinite total curvature (Hoffman and Wei 1993). The helicoid is the conjugate surface to the catenoid, hence locally isometric to the catenoid. It is deformable to a plane. Figure 5 show its configuration.

In the case of curved surface, we can characterize it by two principal curvatures, $\frac{1}{R_1}$ and $\frac{1}{R_2}$ (Figure 6). When the surface is minimum, its mean curvature H is zero.

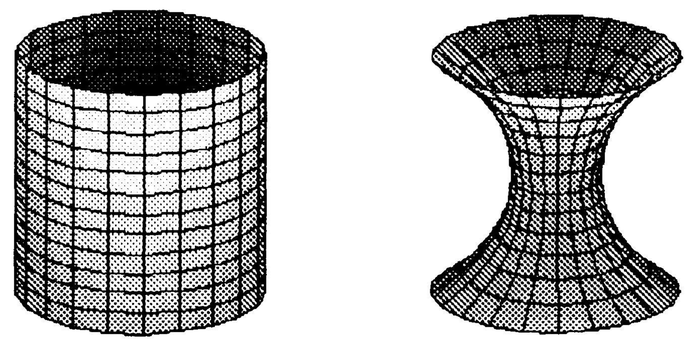

(a) (b)

Figure 3. (a) The mesh is initialized to fit the boundary of the surface. (b) The final result.

That is $\frac{1}{R_1} = -\frac{1}{R_2}$. Taking Figure 3(b) as an example, we measure its two principal curvatures at each node. As we can see in Figure 7(a) and (b), R_1 and R_2 own the similar variations. Note that these two curvatures are orthogonal mutually. The collective and distributive operations of the network are of much benifit to the emulation of the soap film. The initialization of the mesh is skillfully, and will be technical for dificult boundaries. Hopfield model can also be applied in this method by omitting MFT procedure.

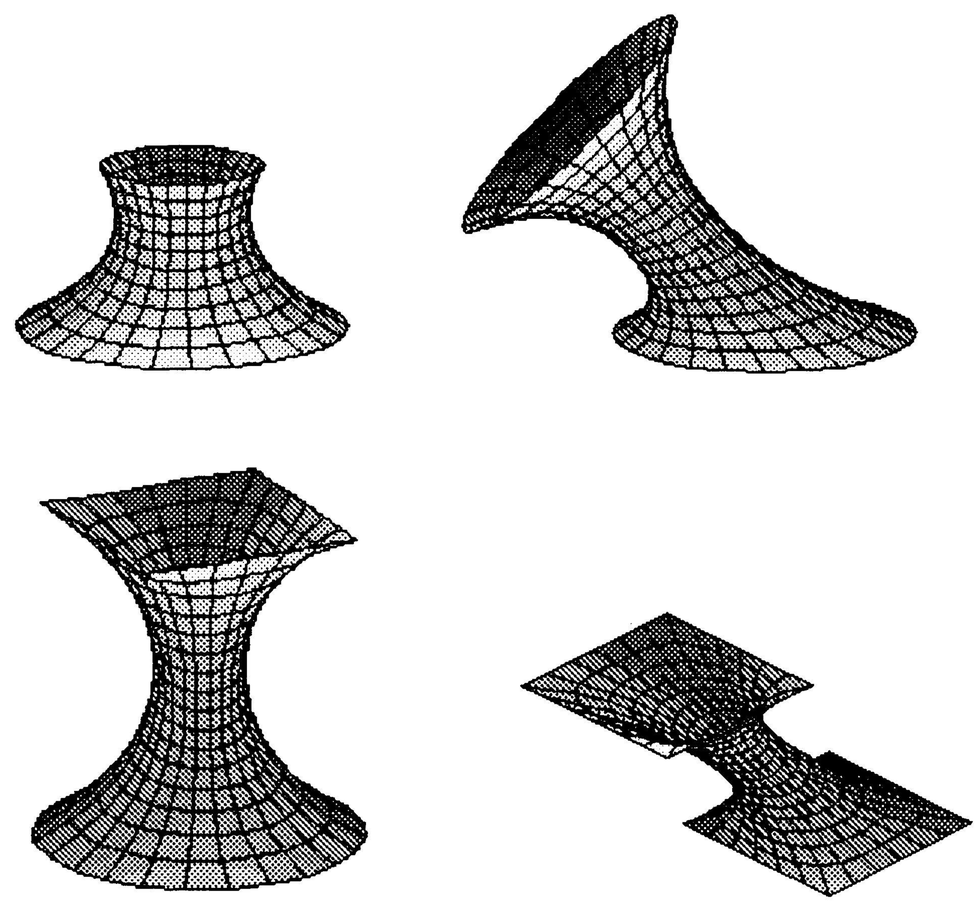

Figure 4. Four variations of the catenoid.

References

[Brakke 92] Brakke, K. A., The Surface Evolver, *Experimental Mathematics*, vol. 1, no. 2, pp. 141–165, 1992.

[Callahan 88] Callahan, M. J., Hoffman, D. & Hoffman, J. T., Computer graphics tools for the study of minimal surfaces, *Communications of the ACM*, vol. 31, no. 6, pp. 648–661, 1988.

[Courant 41] Courant, R. & Robbins, H., *What Is Mathematics ?* Oxford University Press, New York, 1941.

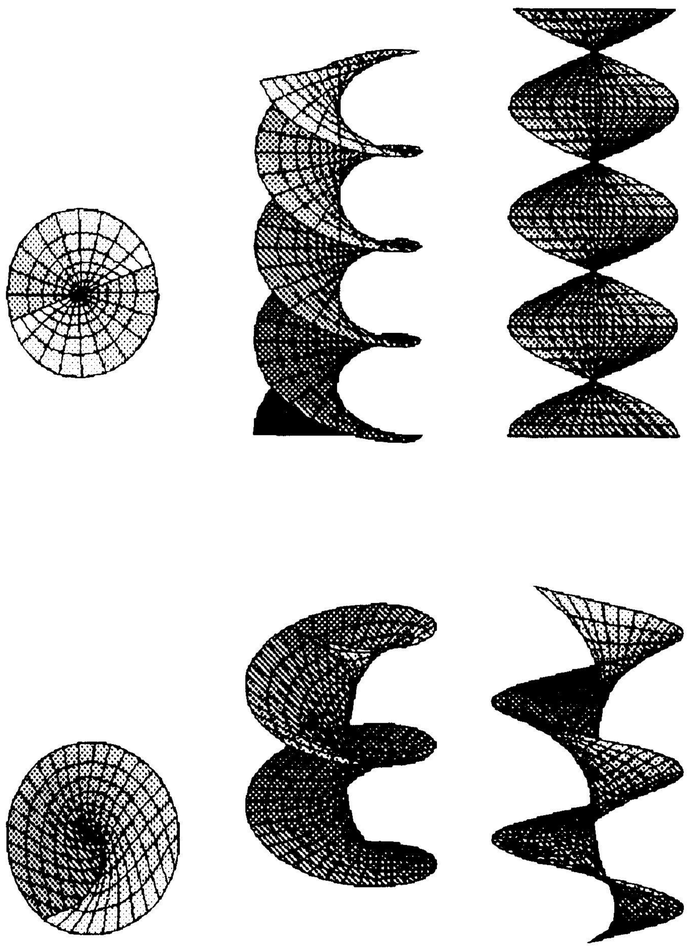

Figure 5. The helicoid. Left picture shows its top view, right picture shows its side view. A type of screw surface.

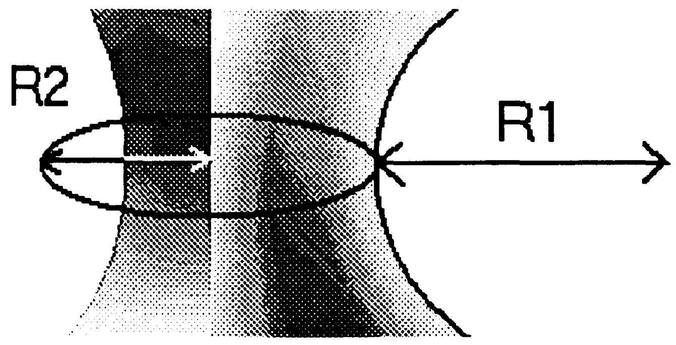

Figure 6. The two principal curvatures of the surface (corresponding to Figure 3(b)).

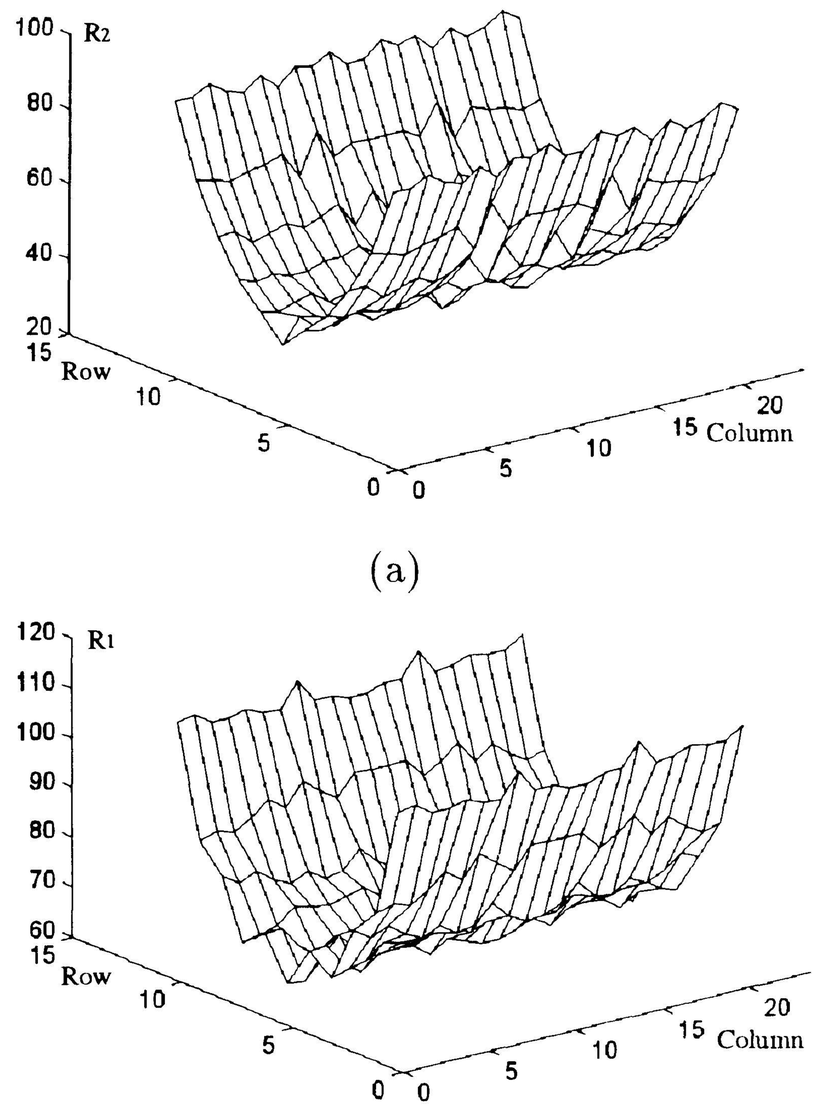

Figure 7. (a)(b) The variations of the two principal curvatures of Figure 3(b).

[Hoffman 90] Hoffman, D. & Meeks, W. H., Minimal surfaces based on the catenoid, *The American Mathematical Monthly*, vol. 97, no. 8, pp. 702–730, 1990.

[Hoffman 93] Hoffman, D., Wei, F. & Karcher, H., Adding handles to the helicoid, *Bulletin of the American Mathematical Society*, vol. 29, no. 1, pp. 77–85, 1993.

[Kass 87] Kass, M., Witkin, A. & Terzopoulos, D., Snakes: active contour models, *Proceedings of IEEE International Conference on Computer Vision*, pp. 259–268, 1987.

[Liou96] Liou, C.- Y., & Chang, Q.- M., Numerical Soap Film for the Steiner Tree Problem, *Proceedings of the International Conference on Neural Information Processing*, ICONIP, vol. 1, pp. 642-647, September, 1996.

[Liou97] Liou, C.- Y., & Chang, Q.- M., Neural Mesh For the Steiner Tree Problem, *Journal of Information Science and Engineering*, vol. 13, no. 2, the 7th article.

[Peterson 89] Peterson, C. & Söderberg, B., A new method for mapping optimization problems onto neural networks, *International Journal of Neural Systems*, vol. 1 no. 1, pp. 3–22, 1989.

[Pinkall 93] Pinkall, U. & Polthier, K., Computing discrete minimal surfaces and their conjugates, *Experimental Mathematics*, vol. 2, no. 1, pp. 15–36, 1993.

[Tsai 93] Tsai, C. T., Sun, Y. N. & Chung, P. C., Minimising the energy of active contour model using a Hopfield network, *IEE Proceedings-E*, vol. 140, no. 6, pp. 297–303, 1993.

[Williams 92] Williams, D. J. & Shah, M., A fast algorithm for active contours and curvature estimation, *CVGIV: Image Understanding*, vol. 55, no. 1, pp. 14–26, 1992.

[Wu82] Wu, F. K., The Potts model, *Reviews of Modern Physics*, vol. 54, no. 1, pp. 235–268, 1982.